nature chemistry

SUPPLEMENTARY INFORMATION

DOI: 10.1038/NCHEM.1442

Use of the interior cavity of the P22 capsid for site-specific initiation of atom-transfer radical polymerization with high-density cargo loading

Janice Lucon[1,2], Shefah Qazi[1,2], Masaki Uchida[1,2], Gregory J. Bedwell[3], Ben LaFrance[1,2], Peter E. Prevelige, Jr.[3], and Trevor Douglas[1,2]*

[1] Chemistry and Biochemistry Department, Montana State University, Bozeman, Montana, 59717

[2] Center for Bio-Inspired Nanomaterials, Montana State University, Bozeman, Montana, 59717

[3] Department of Microbiology, University of Alabama at Birmingham, Birmingham, Alabama, 35294

Contents Page

Additional Methods:

Mutagenesis. The P22(S39C) point mutation was made using established polymerase chain reaction protocols (Qiagen) using pET-11a based plasmids encoding genes for scaffolding and coat protein. The amplified DNA was transformed into E. coli strain BL21 (DE) and selected for ampicillin resistance.[3]

Protein Purification. Transformed BL21 (DE3) *E. coli* were grown in 1L cultures inoculated with 1 mL starter culture at 37°C with vigorous shaking overnight. The bacteria were then centrifuged away from the media at 3700 g for 20 minutes. The cell pellets were resuspended in PBS pH 7.2 and were incubated with DNAse, RNAse, and lysozyme (all Sigma-Aldrich) for 30 minutes on ice. Cells were lysed further by sonication on ice. The cell debris was removed via centrifugation at 12,000 g for 45 minutes. The supernatant was then loaded on a 35% sucrose cushion and centrifuged at 48,000 rpm for 50 minutes in an ultra centrifuge (Sorvall). The resulting virus pellet was resuspended in PBS pH 7.0, spun at 17,000 rpm for 20 minutes to remove particulates and lipid providing 135 mg of P22 procapsid (PC). Scaffold protein was extracted using 0.5 M guanidine-HCl in 4 repeated cycles. The P22 empty shells were then dialyzed against PBS pH 7.0 overnight resulting in 86 mg (64% yield) P22 empty shell (ES). The empty shell P22 was heat treated for 20 min at 65°C to transform the protein into its expanded form as previously described and analyzed.[3] The heat treated samples were purified by pelleting as above, followed by resuspension into PBS pH 7.6 in preparation for protein labeling yielding 58 mg (68% yield form ES) of P22 expanded shell (EX) from 1L of initial *E. coli* culture.

Subunit Mass Spectrometry. Subunit masses of the P22 coat and P22-int macroinitiators were analyzed by ESI-Q-TOF mass spectrometry (Q-TOF Premier, Waters) interfaced to a Waters Acquity UPLC and autosampler. [4] Samples were loaded onto a BioBasic-300 SEC column (5 µm, 250 L x 1.0 mm I.D., Thermo Scientific) and eluted with buffer containing 40% isoproanol, 59.9% water, and 0.1% formic acid isocratically with a rate of 25 µL/min. Mass spectra were acquired in the range of m/z 50-5000 and processed using the MaxEnt 1 algorithm for MassLynx version 4.1 to obtain deconvoluted average masses from multiple charge state distributions.

Transmission Electron Microscopy. The P22-int macroinitiators and P22-polymer composites were imaged by transmission electron microscopy (Leo 912 AB) by negatively staining the sample with 1% uranyl acetate on formvar carbon coated grids. For the diameter measurements 200 particles were measured for each sample.

Denaturing Gel Assay. P22-int macroinitiators and P22-polymer composites were analyzed using SDS-PAGE on 10-20% gradient Tris-glycine gels (Lonza). Fluorescence imaging of the gels was carried out on a Typhoon TRIO (GE Healthcare) gel scanner with excitation at 488 nm and detection at 526 nm. Protein was detected by staining with Coomassie blue.

Native Agarose Gel Assay. P22-int macroinitiators and P22-polymer composites were analyzed on 0.8% native agarose gel using 40 mM Tris-base, 5 mM sodium acetate, 1 mM EDTA, pH 8.2 running buffer and were run for 3 hours at 65 volts. Fluorescence imaging of the gels was carried out on a Typhoon TRIO (GE Healthcare) gel scanner with excitation at 488 nm and detection at 526 nm. Protein was detected by staining with Coomassie blue.

Analytical Ultracentrifugation. Sedimentation velocity experiments were performed in an XL-A ultracentrifuge (Beckman Coulter, Fullerton, CA) using a AN-60Ti rotor. Epon double-sector centerpieces were filled with 390 µL or 400 µL of sample and the corresponding reference buffer, respectively. The samples were centrifuged at 20°C and 5,000-7,000 rpm. Absorbance data were acquired at wavelength of 280nm. The raw data were analyzed using SEDFIT software, implementing the ls-g*(s) model. Input parameters such as buffer density and viscosity were determined using Sednterp software.

Relaxivity Measurements.
T1 measurements were carried out on Anasazi FT-NMR 60MHz (1.41 T) spectrometer for all samples. Each P22-xAEMA-Gd (0.61 mM Gd, 1.3 mg/ml protein) experimental replicate was diluted with 67% D_2O in H_2O to yield a dilution series with concentrations of 0.20, 0.068, 0.023 mM Gd. The longitudinal relaxation rate constant (T1) at each dilution was measured using an inversion recovery pulse sequence (90º pulse width of 6.3 µs with 8 experiments of 1 scan) at 298 K, where the relaxation delay was set to six times the estimated T1 (Supplemental Figure S12 A-C). To attain the actual T1 value, the following equation for T1 relaxation:

$$M_z = A(1-\exp(-t/T1))+B$$

was fit to the experimental data acquired at each dilution where A, B, and T1 were used as fitting parameters.[5] The plot of inverse T1 versus Gd (mM) for the 3 dilutions was used to determine relaxivity values (r1), where relaxivity per Gd is equal to the slope of the line (Supplemental Figure S12 D) and relaxivity per VLP was calculated by multiplying the slope by Gd/VLP.

Supplemental Figures:

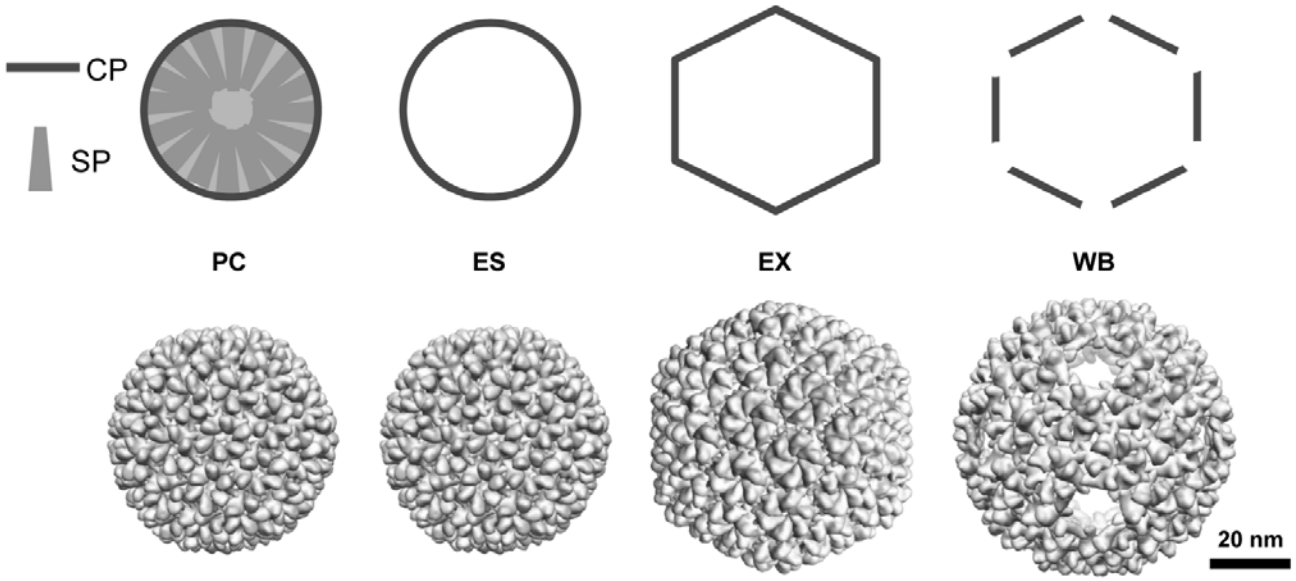

Figure S1: Four unique morphological forms of P22. The coat protein (CP) and scaffold protein (SP) are expressed in *E. coli*. The purified protein architecture is in the procapsid state (PC) containing both CP and SP. After extraction with guanidine•HCl only CP remains in the empty shell (ES) state. If the VLP is heated to 65 ºC the shell enlarges to form the expanded shell (EX) state used in this paper. If instead the ES is heated to 75 ºC the wiffleball (WB) state can be made, where pentons are missing from the icosahedral vertices. PDB ID 3IYI, 2XYZ, 3IYH.

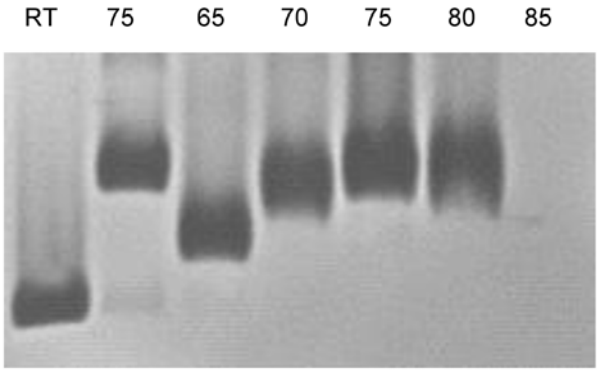

Figure S2: Agarose gel of P22$_{S39C}$-ES heated at different temperatures. Gel labels are heating temperatures in ºC. The states at 65 ºC and 75 ºC correspond to the EX and WB states, respectively. Precipitation occurred while heating at 85 ºC resulting in complete loss of protein.

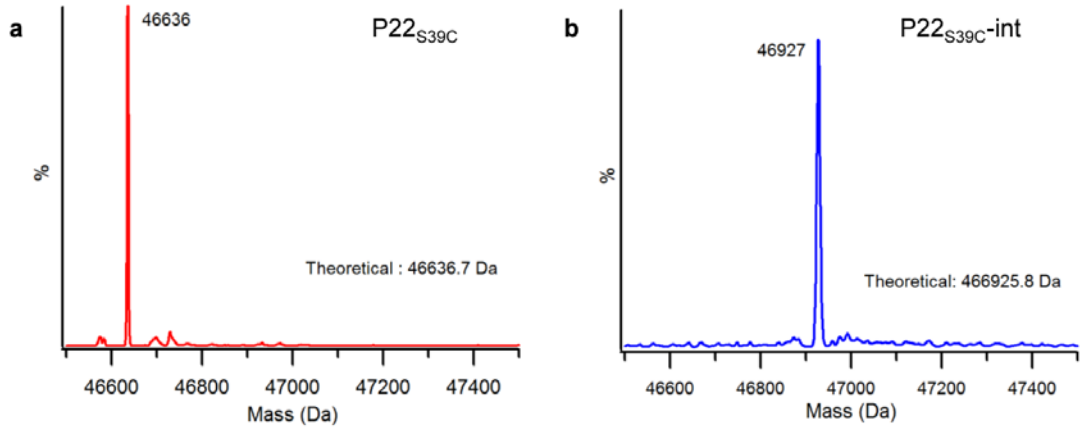

Figure S3: Subunit mass spectrometry characterization of the $P22_{S39C}$ macroinitiator. A) The mass observed is in agreement with the expected mass of the $P22_{S39C}$ mutant B) The only mass observed corresponds to the $P22_{S39C}$-int indicating that all of the subunits have reacted and that there is no significant multiple labeling of the subunits.

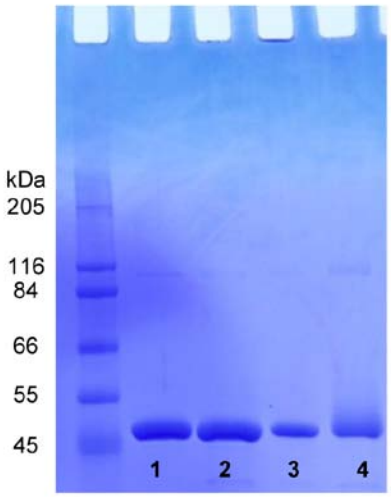

Figure S4: Denaturing gel electrophoresis of P22-polymer samples made with varying amounts of metal catalyst. The amount of catalyst per protein subunit ranged from 0 eq. (lane 1), 10 eq. (lane 2), 40 eq. (lane 3), to 100 eq. (lane 4). Based on this gel 100 eq was determined to be the most effective of these tested conditions.

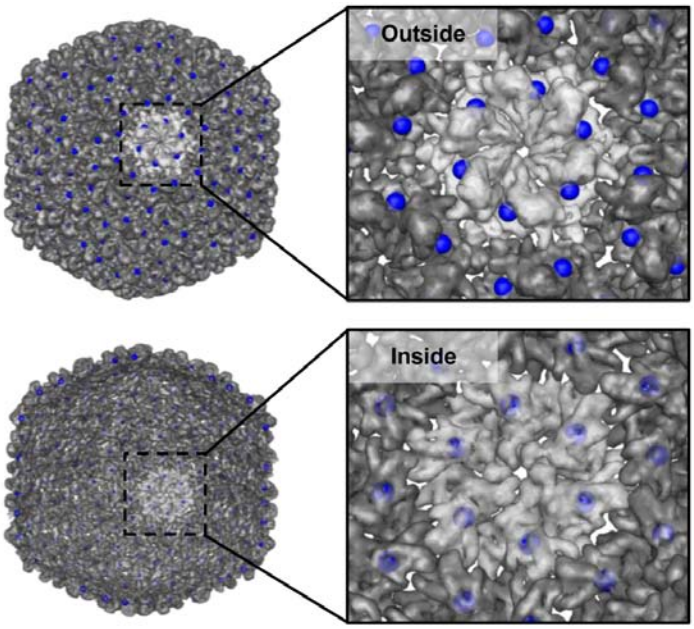

Figure S5: Structural model of the P22 capsid expanded morphology showing the location of the K118C mutation. Location of the modified residue, K118C (in blue), derived from the structural model of P22 using coordination data deposited as PDB file 2XYZ. Both a view of the exterior of the capsid (top) and a half shell cut-away view revealing the interior (bottom) are shown, to illustrate the location of the mutation site.

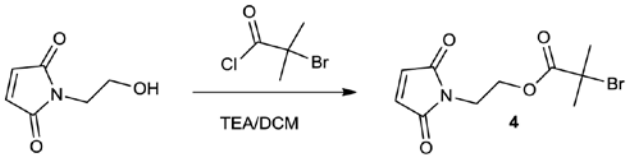

Figure S6: Synthesis of 2-bromoisobutyrate ethoxy maleimide (4). **4** was synthesized by a modification of the procedures previously reported.[1,2] Ethanol-maleimide (200 mg, 1.42 mmol) was mixed on ice with triethylamine (197 ul, 1.42 mmol) in 5 ml dry dichloromethane. 2-bromo-2-methylpropionylbromide (266 ul, 2.13 mmol) was added dropwise. The reaction was allowed to warm to room temperature and was determined by thin layer chromatography to have reached completion after 1.5 hr. The solvent was removed and the product was subsequently cleaned via column chromatography (silica gel, dichloromethane) with a yield of 76%. ^{1}H NMR (500 MHz, $CDCl_3$) δ = 1.87 (s, 6H, CH_3); 3.84 (t, J = 5.5, 2H, NCH_2); 4.31 (t, J = 5.5, 2H, OCH_2); 6.71 (s, 2H, CH_{vinyl}). ^{13}C δ = 30.59 (CH_3), 36.57(NCH_2), 62.88(OCH_2), 134.26(CH_{vinyl}).

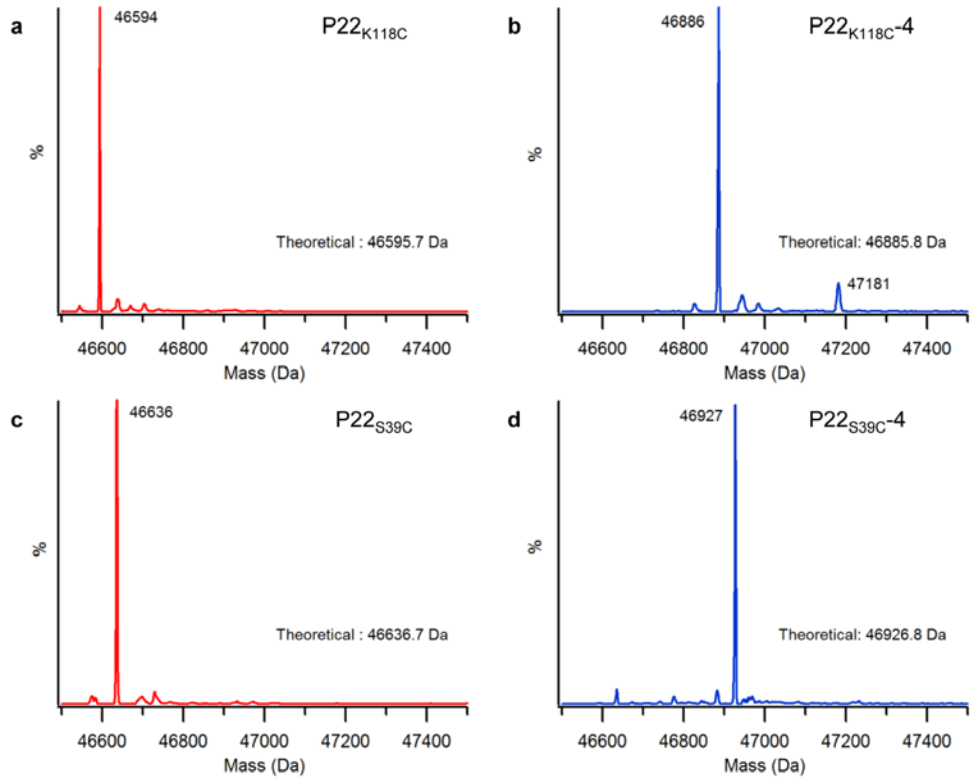

Figure S7: Subunit mass spectrometry characterization of the $P22_{S39C}$-4 and $P22_{K118C}$-4 macroinitiators. A) The mass observed is in agreement with the expected mass of the $P22_{K118C}$ mutant. B) The majority mass observed corresponds to the $P22_{K118C}$-**4** indicating that most of the subunits have reacted and that there is less than 5% double labeling (47181 Da) of the subunits. C) The mass observed is in agreement with the expected mass of the $P22_{S39C}$ mutant D) The only mass observed corresponds to the $P22_{S39C}$-**4** indicating that all of the subunits have reacted and that there is no significant multiple labeling of the subunits.

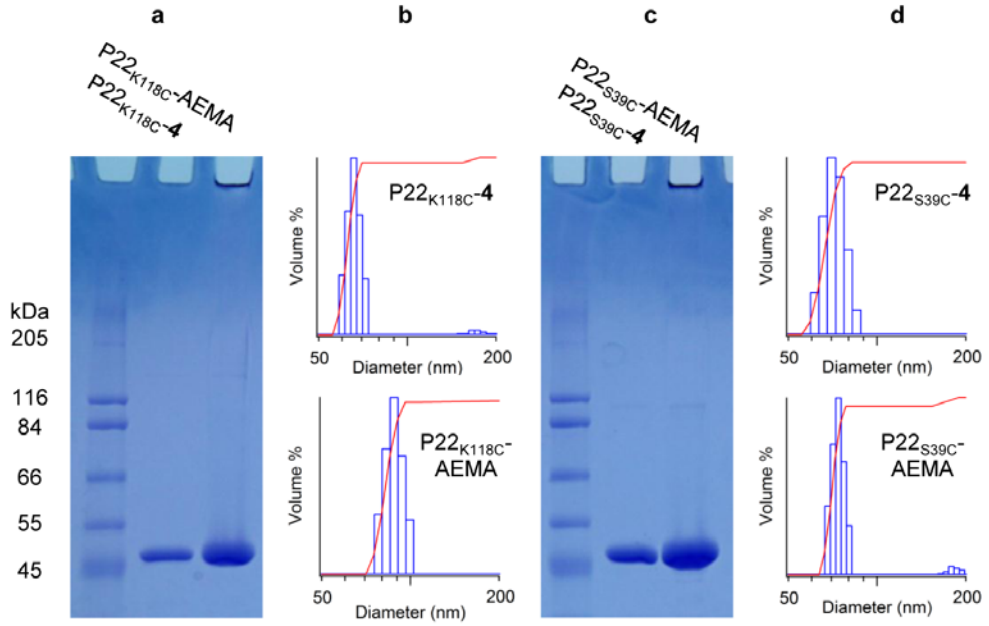

Figure S8: Basic analysis of $P22_{K118C}$-AEMA and $P22_{S39C}$-AEMA. The $P22_{K118C}$-AEMA composite exhibits increased subunit mass, but concomitantly increases in diameter, while the $P22_{S39C}$-AEMA retains its initial diameter. A) $P22_{K118C}$-AEMA analyzed by SDS-PAGE. B) Dynamic light scattering of $P22_{K118C}$-AEMA indicates that at least some of the polymer is on the exterior of the cage through the increase in diameter from 60 ± 3 nm to 81 ± 4 nm. C) $P22_{S39C}$-AEMA analyzed by SDS-PAGE. B) Dynamic light scattering of $P22_{S39C}$-AEMA indicates that the polymer is on the interior of the cage through retention of diameter changing from 72 ± 5 nm to 68 ± 4 nm.

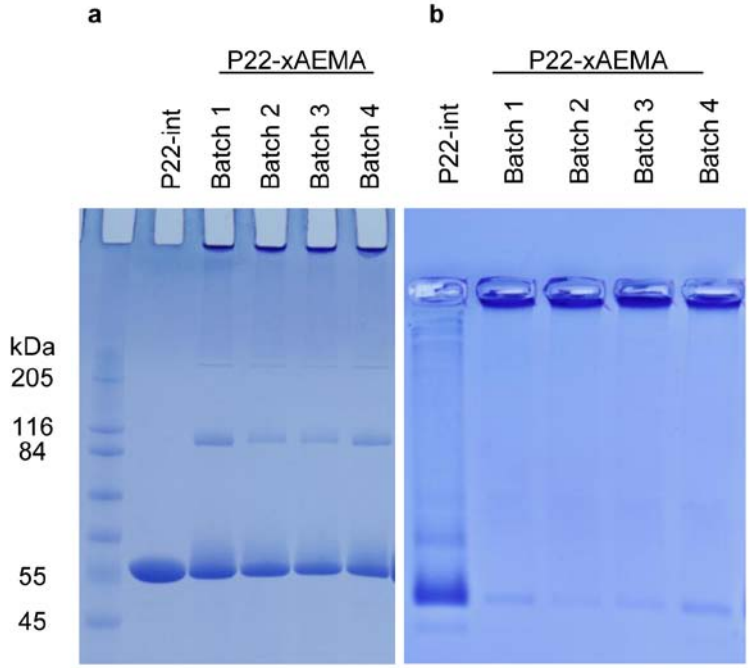

Figure S9: Gel analysis comparison of 4 experimental replicates of the $P22_{S39C}$-xAEMA synthesis. A) When subjected to denaturing gel condition a streak to higher molecular mass and the appearance of dimer due to subunit crosslinking is observed indicating the growth of crosslinked polymer chains on the subunits in each batch. B) When each batch is analyzed by native agarose gel conditions a uniform shift in mobility compared to $P22_{S39C}$-int is observed.

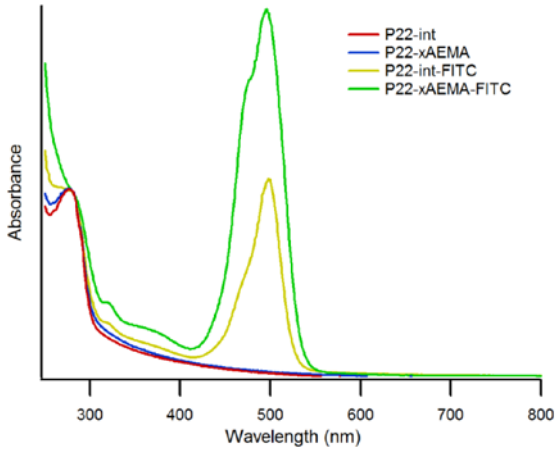

Figure S10: Representative absorbance profiles of the $P22_{S39C}$-int, $P22_{S39C}$-xAEMA, $P22_{S39C}$-int-FITC, and $P22_{S39C}$-xAEMA-FITC. The $P22_{S39C}$-int-FITC is labeled on the intrinsic lysine residues of the protein, while the $P22_{S39C}$-xAEMA-FITC has labeling both on the lysines and the AEMA introduced primary amines. FITC is the contributor to the absorbance at 495 nm, while both the protein-polymer composite and FITC absorb at 280 nm.

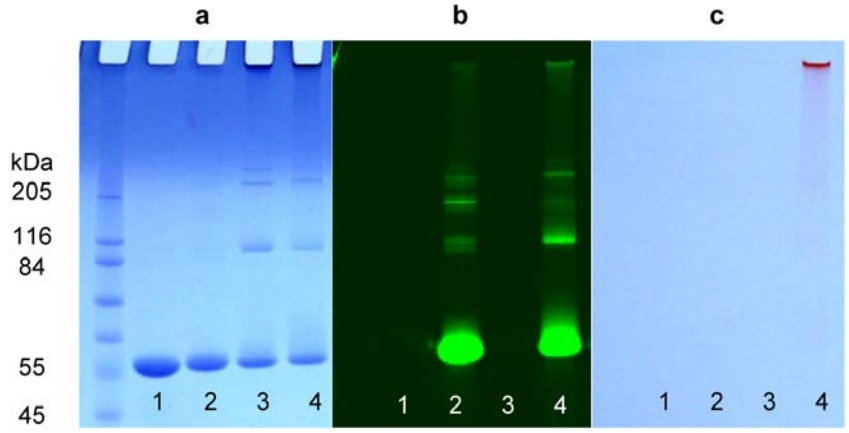

Figure S11: **Verification of FITC covalent attachment by denaturing gel electrophoresis.** Three different views of the same SDS-PAGE denaturing gel electrophoresis of $P22_{S39C}$-int (lane 1), $P22_{S39C}$-int-FITC (lane 2), $P22_{S39C}$-xAEMA (lane 3), and $P22_{S39C}$-xAEMA-FITC (lane 4). A) The gel after Coomassie staining highlighting the protein component of the samples with the unmodified subunit appearing at about 46 kDa and the modified subunits (lanes 3 and 4) streaking to higher molecular weights. B) Both the $P22_{S39C}$-int-FITC and $P22_{S39C}$-xAEMA-FITC subunits are visible when the fluorescent signal from the FITC is visualized. C) The gel under ambient light. Only the $P22_{S39C}$-xAEMA-FITC is visible as orange streak.

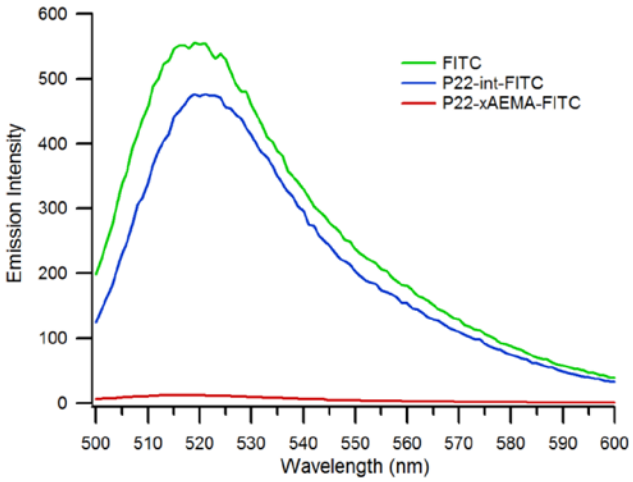

Figure S12: Representative fluorescence emission profiles for FITC labeled samples. In this dataset $P22_{S39C}$-int-FITC and $P22_{S39C}$-xAEMA-FITC compared to free FITC. Each sample had equivalent absorbance at 495 nm and was measured in pH 9.0 buffer. The excitation wavelength was 488 nm and fluorescence emission was detected over the charted range.

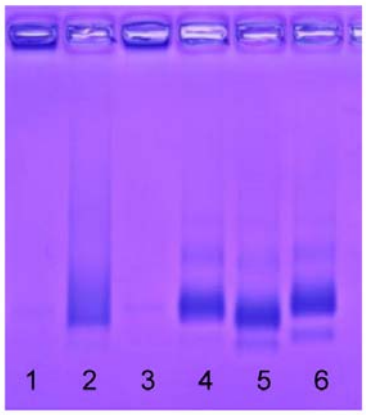

Figure S13: Covalent attachment of Gd-DTPA-NCS monitored by native agarose gel electrophoresis. Native agarose gel analysis of $P22_{S39C}$-xAEMA (lane 1), $P22_{S39C}$-xAEMA-Gd (lane 2), $P22_{S39C}$-xAEMA-magnevist (lane 3), $P22_{S39C}$-int (lane 4), $P22_{S39C}$-int-Gd (lane 5), and $P22_{S39C}$-int-magnevist (lane 6). The attachment of Gd-ATPA-NCS to the polymerized sample has the same effect on electrophoretic mobility as observed in the FITC labeled sample described in Figure 6.

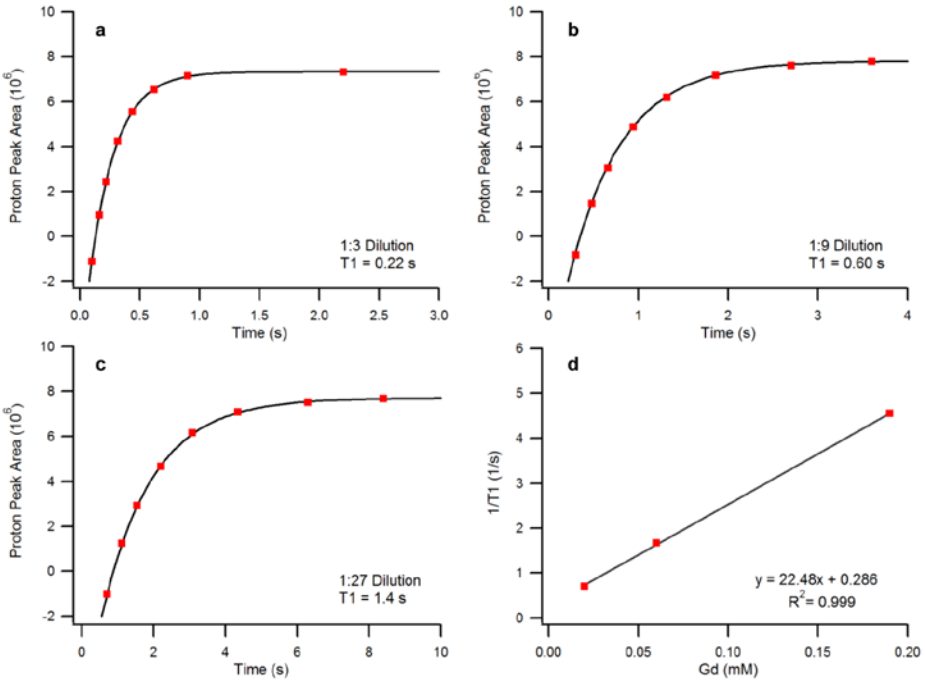

Figure S14: Representative $P22_{S39C}$-xAEMA-Gd data used for relaxivity calculations. A) Raw relaxivity data for the 1:3 dilution sample fit to find T1 at 0.20 mM Gd. B) Raw relaxivity data for the 1:9 dilution sample fit to find T1 at 0.068 mM Gd. C) Raw relaxivity data for the 1:27 dilution sample fit to find T1 at 0.023 mM Gd. D) Plot of 1/T1 values determined in panels A-C fit to determine the ionic relaxivity (r1).

References:

1 Heredia, K. L. *et al*. In situ preparation of protein: "Smart" polymer conjugates with retention of bioactivity. *J. Am. Chem. Soc*. **127**, 16955-16960 (2005).

2 Mantovani, G. *et al*. Design and synthesis of N-maleimido-functionalized hydrophilic polymers via copper-mediated living radical polymerization: A suitable alternative to PEGylation chemistry. *J. Am. Chem. Soc*. **127**, 2966-2973 (2005).

3 Kang, S. *et al*. Implementation of P22 viral capsids as nanoplatforms. *Biomacromolecules* **11**, 2804-2809 (2010).

4 Kang, S. *et al*. Controlled assembly of bifunctional chimeric protein cages and composition analysis using noncovalent mass spectrometry. *J. Am. Chem. Soc*. **130**, 16527-16529 (2008).

5 Mitchell, D. G. & Cohen, M. *MRI Principles*. 2 edn, 10-12 (Saunders, 2004).